Available online at www.sciencedirect.com
SCIENCE DIRECT®
Bioorganic & Medicinal Chemistry 13 (2005) 6803–6809
Bioorganic & Medicinal Chemistry

Verification of the turn at positions 22 and 23 of the β-amyloid fibrils with Italian mutation using solid-state NMR

Yuichi Masuda,[a] Kazuhiro Irie,[a,*] Kazuma Murakami,[a] Hajime Ohigashi,[a] Ryutaro Ohashi,[b] K. Takegoshi,[b] Takahiko Shimizu[c] and Takuji Shirasawa[c]

[a]*Division of Food Science and Biotechnology, Graduate School of Agriculture, Kyoto University, Kitashirakawa Oiwake-cho, Sakyo-ku, Kyoto 606-8502, Japan*
[b]*Department of Chemistry, Graduate School of Science, Kyoto University, Kitashirakawa Oiwake-cho, Sakyo-ku, Kyoto 606-8502, Japan*
[c]*Research Team for Molecular Biomarkers, Tokyo Metropolitan Institute of Gerontology, 35-2 Sakae-cho, Itabashi-ku, Tokyo 173-0015, Japan*

Received 15 June 2005; revised 21 July 2005; accepted 22 July 2005
Available online 22 September 2005

Abstract—The aggregation of 42-mer amyloid β (Aβ42) plays a central role in the pathogenesis of Alzheimer's disease. Our recent research on proline mutagenesis of Aβ42 suggested that the formation of a turn structure at positions 22 and 23 could play a crucial role in its aggregative ability and neurotoxicity. Since E22K-Aβ42 (Italian mutation) aggregated more rapidly and with more potent neurotoxicity than wild-type Aβ42, the tertiary structure at positions 21–24 of E22K-Aβ42 fibrils was analyzed by solid-state NMR using dipolar-assisted rotational resonance (DARR) to identify the 'malignant' conformation of Aβ42. Two sets of chemical shifts for Asp-23 were observed in a ratio of about 2.6:1. The 2D DARR spectra at the mixing time of 500 ms suggested that the side chains of Asp-23 and Val-24 in the major conformer, and those of Lys-22 and Asp-23 in the minor conformer could be located on the same side, respectively. These data support the presence of a turn structure at positions 22 and 23 in E22K-Aβ42 fibrils. The formation of a salt bridge between Lys-22 and Asp-23 in the minor conformer might be a reason why E22K-Aβ42 is more pathogenic than wild-type Aβ42.
© 2005 Elsevier Ltd. All rights reserved.

1. Introduction

Alzheimer's disease (AD) and cerebral amyloid angiopathy (CAA) are characterized by the deposition of amyloid fibrils consisting mainly of 40- and 42-mer peptides (Fig. 1) called amyloid β (Aβ) peptides (Aβ40, Aβ42).[1] Since the aggregation (fibrillation) of Aβ peptides is closely related to the pathogenesis of AD, elucidation of the precise tertiary structure of Aβ fibrils is urgently needed to understand the aggregation mechanism and to develop new agents that inhibit the aggregation.

Previous studies have shown that Aβ fibrils possess a cross-β structure, in which β-strands run perpendicular to the fiber axis[2] and form an intermolecular parallel β-sheet in both Aβ40 and Aβ42.[3,4] Aβ fibrils are 70–120 Å in diameter and composed of several protofilaments, which are 30–60 Å in diameter.[2,5,6] If full-length Aβ molecules were included in an extended β-strand, it would be 139 Å for Aβ40 and 146 Å for Aβ42.[2] Hence, Aβ40 and Aβ42 need to have at least one turn or bend structure to corroborate these data. The structure of Aβ fibrils at high resolution has remained elusive because X-ray crystallography and liquid-state NMR cannot be applied to non-crystalline and insoluble Aβ fibrils. Solid-state NMR, which can measure a non-crystalline powder, is a fairly effective method to analyze the structure. An analysis of Aβ40 fibrils using solid-state NMR has recently been reported.[7] However, there are few reports on the structure of Aβ42 fibrils whose aggregative ability and neurotoxicity are considerably greater than those of Aβ40.

Systematic replacement with proline in peptides is a promising method for predicting the secondary structure.[8] Prolines are rarely present in β-sheets, whereas they can be easily accommodated in a turn or a bend

Keywords: Amyloid β; Solid-state NMR; Italian mutation; Turn.
* Corresponding author. Tel.: +81 75 753 6282; fax: +81 75 753 6284; e-mail: irie@kais.kyoto-u.ac.jp

0968-0896/$ - see front matter © 2005 Elsevier Ltd. All rights reserved.
doi:10.1016/j.bmc.2005.07.071

```
                    1         10        20        30        42
wild-type Aβ42 :    DAEFRHDSGY EVHHQKLVFF AEDVGSNKGA IIGLMVGGVVIA
E22K-Aβ42 (Italian) : DAEFRHDSGY EVHHQKLVFF AKDVGSNKGA IIGLMVGGVVIA
```

Figure 1. Structure of wild-type Aβ42 and E22K-Aβ42 (Italian).

structure.[9] Our recent research on the systematic replacement of Aβ42 with prolines showed that only E22P-Aβ42 among the mutants altered at positions 15–32 aggregated considerably faster and with stronger neurotoxicity than wild-type Aβ42.[10–12] In addition, we found that CAA-related Aβ42 mutants, such as E22K- and E22Q-Aβ42 (Italian and Dutch mutations), aggregated far more rapidly than wild-type Aβ42.[12–14] Since Lys-Asp and Gln-Asp sequences are frequently found in a turn,[9] the formation of a turn structure at positions 22 and 23 might be requisite for the potent aggregative ability and neurotoxicity of Aβ peptides (Fig. 2A). Recent proline mutagenesis of Aβ40 also showed that the formation of a turn structure at positions 22 and 23 enhanced the aggregative ability (Fig. 2B).[15] However, the position of this turn is slightly different from that of Aβ40 fibrils determined by solid-state NMR,[7] in which the residues at positions 25–29 adopt a bend structure (Figs. 2C and D). We postulated the existence of a 'malignant' conformation (Figs. 2A and B) other than the physiological conformation (Figs. 2C and D). The 'malignant' conformation is defined as the conformation that possesses potent aggregative ability and neurotoxicity. Since E22K-Aβ42 has the likely potential to adopt 'malignant' conformation, proportion of the 'malignant' conformers may be larger in E22K-Aβ42 fibrils than in wild-type Aβ42 fibrils. To identify the 'malignant' conformation of Aβ peptides, which is closely related to the pathogenesis of CAA and AD, we analyzed the tertiary structure at positions 21–24 of the E22K-Aβ42 fibrils using solid-state NMR.

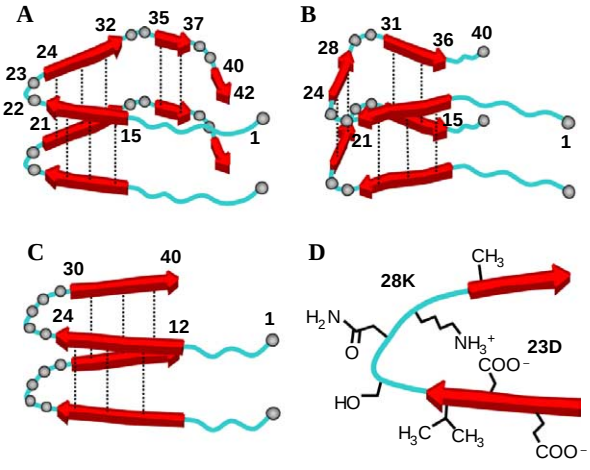

Figure 2. Structural model of the fibrils of wild-type Aβ42 deduced from a systematic replacement with proline by us (A),[11] that of wild-type Aβ40 by Williams et al. from a systematic replacement with proline (B),[15] that of wild-type Aβ40 by Petkova et al. using solid-state NMR (C),[7] and a detail of the bend structure stabilized by a salt bridge between Asp-23 and Lys-28 in wild-type Aβ40 proposed by Petkova et al. (D).[7] (A and B) imply a 'malignant' conformation of each Aβ peptide, whereas (C and D) might be a physiological conformation of Aβ40 in the fibrils. Dotted lines show intermolecular β-sheets.

2. Results and discussion

2.1. Synthesis of E22K-Aβ42 labeled with ^{13}C and ^{15}N

Two kinds of E22K-Aβ42 were prepared in this study: one uniformly labeled with ^{13}C and ^{15}N at positions 21–24 and one where Ala-21 and Lys-22 were uniformly labeled with ^{13}C and ^{15}N, and only C_γ of Asp-23 was labeled with ^{13}C. These peptides were synthesized with a peptide synthesizer of continuous flow-type (Pioneer™) using HATU[16] as an effective coupling activator for Fmoc chemistry.[10–14,17] After cleavage from the resin, the crude peptides were purified by HPLC under alkaline conditions (CH_3CN–0.1% NH_4OH), as reported previously.[10–14] Although the purification of E22K-Aβ42 was extremely difficult, the labeled peptides were successfully obtained in a highly pure form. The total yield of the peptides was about 6%.

2.2. Fibril formation of E22K-Aβ42 labeled with ^{13}C and ^{15}N

We prepared three kinds of E22K-Aβ42 fibrils in this study; E22K-Aβ42 uniformly labeled with ^{13}C and ^{15}N at positions 21–24 diluted with unlabeled E22K-Aβ42 in a ratio of 1:2 (33% labeled E22K-Aβ42), E22K-Aβ42 uniformly labeled with ^{13}C and ^{15}N at positions 21–24 (100% labeled E22K-Aβ42), and E22K-Aβ42 where Ala-21 and Lys-22 were uniformly labeled with ^{13}C and ^{15}N, and only C_γ of Asp-23 was labeled with ^{13}C, were aggregated, respectively, to give each E22K-Aβ42 fibril. The 33% labeled E22K-Aβ42 fibrils were prepared to eliminate the intermolecular ^{13}C–^{13}C correlations. Fibril formation of each peptide sample was evaluated by transmission electron microscopy after a 48-h incubation at 37 °C. As shown in Figure 3, typical fibril formation was confirmed. The morphology of these fibrils resembled that of wild-type Aβ42 well.

2.3. Assignment of the chemical shifts of E22K-Aβ42 labeled with ^{13}C and ^{15}N

The E22K-Aβ42 fibrils described above were analyzed using dipolar-assisted rotational resonance (DARR) [18,19] that enables a broadband ^{13}C–^{13}C correlation 2D experiment. The pulse sequence is shown in Figure 4. The ^{13}C chemical shifts of Asp-23 and Val-24 were assigned from the 2D DARR spectrum of 33% labeled E22K-Aβ42 fibrils at the mixing time of 20 ms (Fig. 5, Table 1), most cross-peaks of which were ascribable to the directly bonded carbon pairs. The ^{13}C chemical shifts of Ala-21 and Lys-22 were assigned unambiguously

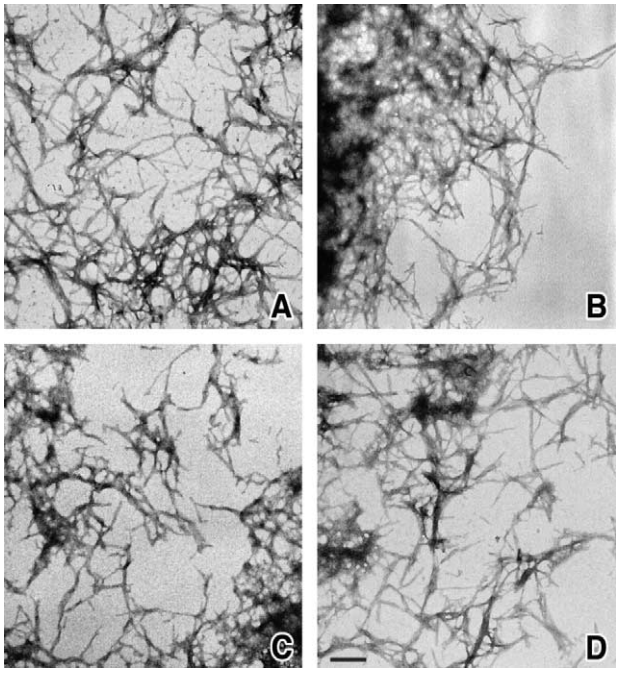

Figure 3. Transmission electron micrographs of negatively stained preparations of the fibrils formed by E22K-Aβ42 labeled with ^{13}C and ^{15}N. Each Aβ peptide (25 μM) was incubated in 50 mM sodium phosphate buffer (pH 7.4) containing 100 mM NaCl at 37 °C for 48 h. (A) Wild-type Aβ42. (B) Unlabeled E22K-Aβ42. (C) E22K-Aβ42 uniformly labeled with ^{13}C and ^{15}N at positions 21–24. (D) E22K-Aβ42 where Ala-21 and Lys-22 were uniformly labeled with ^{13}C and ^{15}N, and C_γ of Asp-23 was labeled with ^{13}C.

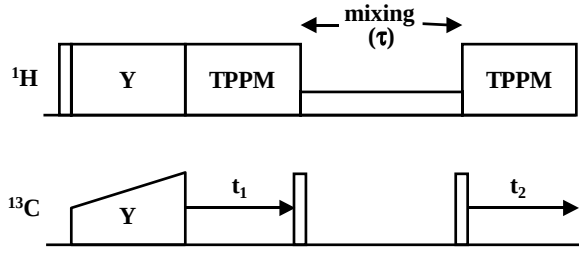

Figure 4. Pulse sequence for the DARR experiment.

from the 2D DARR spectrum (τ = 500 ms) of E22K-Aβ42 fibrils where Ala-21 and Lys-22 were uniformly labeled with ^{13}C and ^{15}N, and only C_γ of Asp-23 was labeled with ^{13}C (Fig. 6, Table 1), in which the intra-residual cross-peaks of Ala-21 and Lys-22 were fairly clear. It is noteworthy that two sets of chemical shifts were observed only for Asp-23 in an intensity-ratio of about 2.6:1. This indicates that Asp-23 exists in two conformations, which were designated as the major and the minor conformers, respectively. On the other hand, only one set of chemical shifts was obtained for Ala-21, Lys-22, and Val-24, suggesting that they might be packed tightly in the fibrils.

2.4. Estimation of the secondary structure at positions 21–24 of E22K-Aβ42

It is known that the deviations of the $^{13}C_\alpha$ chemical shifts, relative to their corresponding random coil values ($\Delta\delta = \delta_{observed} - \delta_{random\ coil}$), are regarded as a particularly useful and sensitive parameter to predict the secondary structure and are positive in the α-helix and negative in the β-sheet, respectively.[20] As shown in Table 1, $\Delta\delta$ values of $^{13}C_\alpha$ at Ala-21 (−2.8), Lys-22 (−2.9), and Val-24 (−3.2) are negative, while those of $^{13}C_\alpha$ at Asp-23 (+0.8 and +1.9) are positive, indicating the existence of a turn, which separates one β-strand including Ala-21 and Lys-22 from the other including Val-24.

2.5. Analysis of the tertiary structure at positions 21–24 of E22K-Aβ42

To analyze the turn structure more accurately, a 2D DARR spectrum at the mixing time of 500 ms was measured using the 33% labeled E22K-Aβ42 fibrils that were prepared to suppress the intermolecular signals. Similar results were obtained using the 100% labeled E22K-Aβ42 fibrils (data not shown). When the mixing time is 500 ms, recoupling of spatially remote carbons up to 5–6 Å occurs. As shown in Figure 7A, a significant cross-peak between C_γ of Asp-23 (major) and a methyl carbon of Ala-21 and/or Val-24 is observed (arrow 1). Precise assignment was difficult because of the similarity in their chemical shifts: C_β of Ala-21 (δ18.9) and C_γ of Val-24 (δ18.0). Although C_γ of Asp-23 (major and/or minor) is likely to have cross-peaks with C_γ and C_δ of Lys-22 (Fig. 7, hatched area of the slice spectra), these peaks could not be identified accurately because of the weak intensity compared to the other peaks.

To remove this signal-overlapping, E22K-Aβ42 fibrils where Ala-21 and Lys-22 were uniformly labeled with ^{13}C and ^{15}N, and C_γ of Asp-23 was labeled with ^{13}C, were analyzed by the 2D DARR experiment at the mixing time of 500 ms (Fig. 7B). In this experiment, we did not dilute the labeled peptide with the corresponding unlabeled peptide since we confirmed that cross-peaks between the intermolecular carbons were much weaker than those of intramolecular carbons in the experiment comparing the 100% labeled E22K-Aβ42 fibrils with the 33% labeled E22K-Aβ42 fibrils. The spectrum showed no cross-peaks between C_γ of Asp-23 (major) and C_β of Ala-21, indicating that the significant cross-peak in Figure 7A (arrow 1) is ascribable to that between C_γ of Asp-23 (major) and that of Val-24. It is possible that the cross-peak (arrow 1) arises from the ^{13}C–^{13}C relay. However, no significant cross-peaks between C_γ (δ177.7) of Asp-23 (major) and C_β (δ32.7) or C_α (δ57.4) of Val-24 were observed, indicating that the cross-peak (arrow 1) reflects a spatial interaction between C_γ of Asp-23 (major) and that of Val-24. These results suggest that the side chains of Asp-23 and Val-24 in the major conformer could be close to each other.

On the other hand, clear cross-peaks between C_γ and C_δ of Lys-22 and C_γ of Asp-23 (minor) were observed (Fig. 7B, arrows 2 and 3). These peaks do not arise from the ^{13}C–^{13}C relay in the labeling pattern where only C_γ of Asp-23 is labeled with ^{13}C. The relay mechanism can also be negated due to the absence of the cross-peak between C_β of Lys-22 and C_γ of Asp-23. Since the cross-peaks between C_γ and C_δ of Lys-22 and C_γ of Asp-23

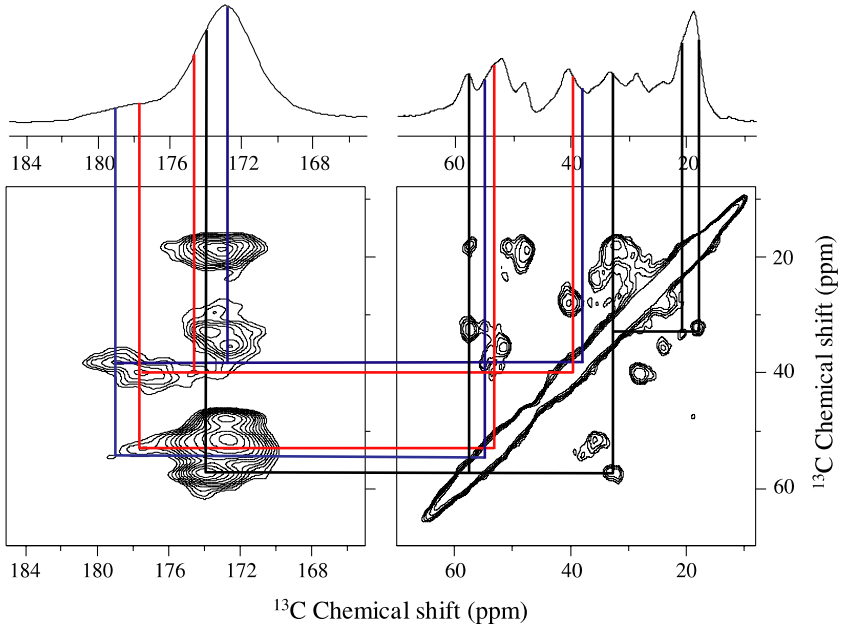

Figure 5. 2D DARR spectrum (τ = 20 ms) of 33% labeled E22K-Aβ42 fibrils in the carbonyl and aliphatic region. Total number of scans was 163,840. 1D ^{13}C CP-MAS spectrum in each region is shown above the 2D spectrum. Assignment paths of Asp-23 and Val-24 are shown in the spectrum: red line, Asp-23 (major); blue line, Asp-23 (minor); black line, Val-24.

Table 1. ^{13}C Chemical shifts [δ (ppm)] of E22K-Aβ42 fibrils[a]

Residue	C=O	C_α	C_β	C_γ	C_δ	C_ε
Ala-21	172.9	48.1	18.9			
	(176.2)[b]	(50.9)	(17.5)			
Lys-22	173.0	51.7	35.8	24.0	28.6	40.6
	(175.0)	(54.6)	(31.5)	(23.1)	(27.4)	(40.3)
Asp-23 (major)[c]	174.5	53.4	40.0	177.7		
Asp-23 (minor)	172.7	54.5	38.2	179.1		
	(174.7)	(52.6)	(39.5)	(178.4)		
Val-24	174.0	57.4	32.7	18.0, 20.8		
	(174.7)	(60.6)	(31.3)	(18.7, 19.5)		

[a] TMS was used as an external standard. The uncertainties of all the values were within 0.3 ppm.
[b] Values in parentheses are chemical shifts in random-coil, adjusted to the TMS reference.[25]
[c] The ratio of the major and minor conformers was about 2.6:1.

(minor) were stronger than those between C_α and C_β of Lys-22 and C_γ of Asp-23 (minor), the side chains of Lys-22 and Asp-23 in the minor conformer would be close to each other. This implies that Lys-22 and Asp-23 in the minor conformer could form a salt bridge.

On the basis of these results along with a requirement for the parallel β-sheet at positions 21 and 34,[4] we deliberated on the structure at positions 21–24 in the E22K-Aβ42 fibrils. If this region were in a parallel β-sheet, adjoining side chains would face in opposite directions to each other and the distance of adjoining side chains among their carbons would be long. However, our present data suggest that the side chains of Asp-23 and Val-24 in the major conformer, and those of Lys-22 and Asp-23 in the minor conformer, are proximate to each other, respectively (Figs. 8A and B). It is reasonable that these side chains are located outside the turn structure to avoid steric hindrance. The side chain of Ala-21 seems to be opposite to that of Lys-22 since no significant cross-peaks between the side chains of Ala-21 and Lys-22 were observed in the 2D DARR spectra at the mixing time of 500 ms (Fig. 6). A small methyl group of Ala-21 inside the turn would be preferable to avoid steric hindrance.

Our present results support the presence of the turn structure at positions 22 and 23 of E22K-Aβ42 fibrils. This turn structure might also exist in E22K-Aβ40 because we have previously shown that E22P-Aβ40 and E22K-Aβ40 exhibited greater aggregative ability and neurotoxicity than wild-type Aβ40.[10–12,14] However, the position of this turn is slightly different from that in the wild-type Aβ40 fibrils determined by Petkova et al. using solid-state NMR (Fig. 2C).[7] In their model, residues at positions 25–29 adopt a bend structure, which is stabilized by a salt bridge between the carboxyl group of Asp-23 and the amino group of Lys-28 (Fig. 2D). In our model of the minor conformer of E22K-Aβ42 fibrils, the carboxyl group of Asp-23 could

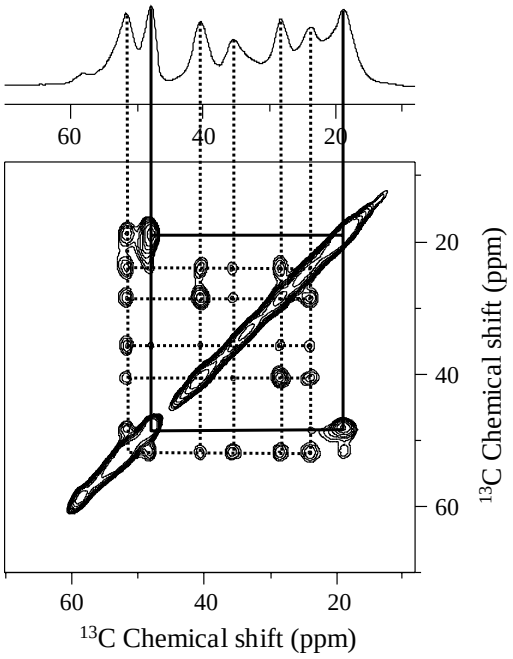

Figure 6. 2D DARR spectrum (τ = 500 ms) of E22K-Aβ42 fibrils where Ala-21 and Lys-22 were uniformly labeled with ^{13}C and ^{15}N, and C_γ of Asp-23 was labeled with ^{13}C in the aliphatic region. Total number of scans was 131,072. 1D ^{13}C CP-MAS spectrum in this region is shown above the 2D spectrum. Assignment paths of Ala-21 and Lys-22 are shown in the spectrum: solid line, Ala-21; dotted line, Lys-22.

form a salt bridge with the amino group of Lys-22 (Fig. 8B). This salt bridge would promote the formation of the turn structure at positions 22 and 23. Since such an ionic interaction is not possible in wild-type Aβ42, E22K-Aβ42 might have a propensity to form the turn structure at positions 22 and 23 to aggregate more rapidly and with more potent neurotoxicity than wild-type Aβ42. On the other hand, such an ionic interaction does not occur at Lys-22 and Asp-23 of the major conformer (Fig. 8A). However, the tertiary structure at positions 21–24 in the major conformer would be similar to that in the minor conformer because only one set of chemical shifts was observed for Ala-21, Lys-22, and Val-24. Since the interaction stabilizing the major conformer might exist in the region other than positions 21–24, structural analysis of the neighboring region is needed.

3. Conclusion

In this study, we verified the presence of the turn structure at positions 22 and 23 of E22K-Aβ42 fibrils using solid-state NMR. The formation of a turn structure at positions 22 and 23 in E22K-Aβ42 fibrils could be closely related to the pathogenesis of CAA and AD. We speculate that such a 'malignant' conformer also exists in wild-type Aβ42 as a minor component since the fibrils of E22P-Aβ42 with rapid aggregative ability and potent

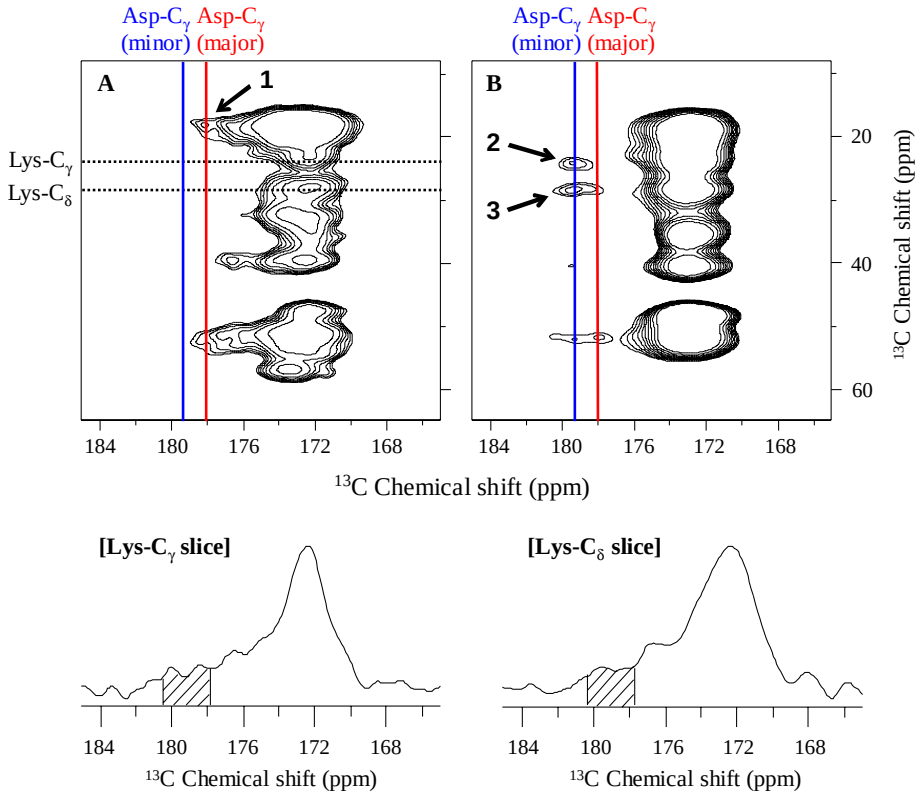

Figure 7. 2D DARR spectrum (τ = 500 ms) of E22K-Aβ42 fibrils in the carbonyl region. (A) E22K-Aβ42 uniformly labeled with ^{13}C and ^{15}N at positions 21–24 was diluted with unlabeled E22K-Aβ42 in a ratio of 1:2 (33% labeled E22K-Aβ42) (total number of scans = 163,840). 1D slices through C_γ and C_δ of Lys-22 (dotted lines in A) are shown below. Hatched areas in the slice spectra indicate the cross-peaks between C_γ of Asp-23 (major and/or minor), and C_γ and C_δ of Lys-22. (B) E22K-Aβ42 where Ala-21 and Lys-22 were uniformly labeled with ^{13}C and ^{15}N, and C_γ of Asp-23 was labeled with ^{13}C (total number of scans = 131,072). Assignment paths of C_γ of Asp-23 are shown in the spectra: red line, C_γ of Asp-23 (major); blue line, C_γ of Asp-23 (minor). Arrows in the spectra indicate the significant cross-peaks: 1, the cross-peak between C_γ of Asp-23 (major) and that of Val-24; 2, that between C_γ of Lys-22 and C_γ of Asp-23 (minor); 3, that between C_δ of Lys-22 and C_γ of Asp-23 (minor).

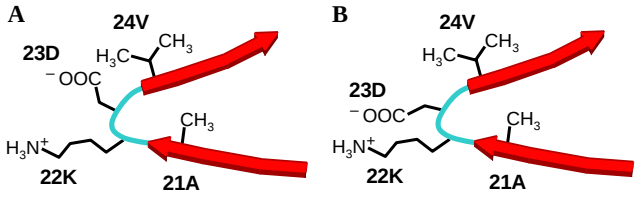

Figure 8. (A) Possible structure of the major conformer at positions 21–24 of E22K-Aβ42 fibrils. (B) Possible structure of the minor conformer at positions 21–24 of E22K-Aβ42 fibrils. In the minor conformer, the formation of a salt bridge between the amino group of Lys-22 and the carboxyl group of Asp-23 might stabilize the turn structure at positions 22 and 23.

neurotoxicity are more thermodynamically stable than those of wild-type Aβ42.[11] Even if the proportion of 'malignant' conformers were small in wild-type Aβ42, it should play a crucial role in triggering the aggregation as a seed in the early onset of CAA and AD. A structural analysis of wild-type Aβ42 fibrils using solid-state NMR is also in progress in our laboratory.

4. Experimental

4.1. General procedures

The following spectroscopic and analytical instruments were used: ^{1}H and ^{13}C NMR in solution, Bruker AVANCE 400 and AC300 (ref. TMS); MS, JEOL JMS-600H; peptide synthesizer, Pioneer™ peptide synthesizer (Applied Biosystems, Foster City, CA); HPLC, Waters 600E multisolvent delivery system with a 2487 UV dual λ absorbance detector; matrix-assisted laser desorption/ionization time-of-flight mass spectrometry (MALDI-TOF-MS), Voyager-DE PRO (Applied Biosystems); electron microscope, Hitachi H-7500 electron microscope; solid-state NMR spectrometer, Chemagnetics Infinity NMR spectrometer, and Chemagnetics 3.2 mm magic angle spinning (MAS) probe. MALDI-TOF-MS was measured, as reported previously.[17] Wakogel™ C-200 (silica gel, Wako Pure Chemical Industries) and Silica gel 60 (0.040–0.063 mm) (MERCK) were used for column chromatography. HPLC was carried out on a Develosil-packed column ODS-UG-5 (20-mm inner diameter × 150-mm) (Nomura Chemicals, Seto, Japan).

L-Ala-$^{13}C_3$, ^{15}N, *N*-(9-fluorenyl)methoxycarbonyl (Fmoc) derivative and L-Val-$^{13}C_5$, ^{15}N, *N*-Fmoc derivative were purchased from Cambridge Isotope Laboratories, Inc. L-Asp-$^{13}C_4$, ^{15}N was purchased from Spectra Stable Isotopes, MD, USA. L-Lys-$^{13}C_6$, $^{15}N_2$ and L-Asp-4-^{13}C were purchased from Taiyo Nippon Sanso Corporation, Tokyo, Japan. HATU,[16] piperidine, Fmoc amino acids, Fmoc-Ala-polyethylene glycol-polystyrlene support (PEG-PS) resin, and *N*,*N*-diisopropylethylamine (DIPEA) were purchased from Applied Biosystems. *N*,*N*-dimethylformamide (DMF), trifluoroacetic acid, 1,2-ethanedithiol, thioanisole, *m*-cresol, and diethyl ether (peroxide free) were purchased from Sigma.

4.2. Preparation of protected amino acids labeled with ^{13}C and ^{15}N

L-Lys-$^{13}C_6$, $^{15}N_2$, α-*N*-Fmoc, ε-*N*-*t*-butoxycarbonyl derivative was synthesized, as reported previously.[21] The crude compound was purified by column chromatography on Wakogel™ C-200 using hexane and increasing amounts of EtOAc containing 0.1% acetic acid. Recrystallization from hexane–EtOAc gave the final product as colorless leaflets in 55% yield. The structure was confirmed by ^{1}H NMR, ^{13}C NMR, and mass measurements.

L-Asp-$^{13}C_4$, ^{15}N, *N*-Fmoc, β-*O*-*t*-butyl ester and L-Asp-4-^{13}C, *N*-Fmoc, β-*O*-*t*-butyl ester were synthesized, as reported previously.[22] The crude product was purified by column chromatography on Silica gel 60 using hexane and increasing amounts of EtOAc containing 0.15% acetic acid. Recrystallization from hexane–EtOAc gave the final product as colorless needles in 27% and 22% yields, respectively. Their structures were confirmed by ^{1}H NMR, ^{13}C NMR, and mass measurements.

4.3. Synthesis of E22K-Aβ42 labeled with ^{13}C and ^{15}N

Each E22K-Aβ42 (Fig. 1) labeled with ^{13}C and ^{15}N was synthesized in a stepwise fashion on 0.1 mmol of preloaded Fmoc-Ala-PEG-PS resin by Pioneer™ using the Fmoc method, as reported previously.[10–14,17] The coupling reaction was carried out using Fmoc amino acid (0.4 mmol), HATU (0.4 mmol), and DIPEA (0.8 mmol) in DMF for 30 min. After each coupling reaction, the N-terminal Fmoc group was removed with 20% piperidine in DMF.

After completion of the chain elongation, each peptide resin washed with DMF and CH_2Cl_2 was treated with a cocktail containing trifluoroacetic acid, *m*-cresol, ethanedithiol, and thioanisole for final deprotection and cleavage from the resin. After shaking at room temperature for 2 h, the crude peptide precipitated by diethyl ether was purified by HPLC under alkaline conditions, as reported previously.[10–14] Lyophilization gave a corresponding pure E22K-Aβ42, the purity of which was confirmed by HPLC (>98%). Each purified peptide exhibited satisfactory mass spectral data by MALDI-TOF-MS: for E22K-Aβ42 uniformly labeled with ^{13}C and ^{15}N at positions 21–24 (MH^+, average molecular mass; observed 4536.13, calculated 4536.99) and for E22K-Aβ42 where Ala-21 and Lys-22 were uniformly labeled with ^{13}C and ^{15}N, and only C_γ of Asp-23 was labeled with ^{13}C (MH^+, average molecular mass; observed 4527.83, calculated 4527.03).

4.4. Fibril formation of E22K-Aβ42 labeled with ^{13}C and ^{15}N

Each E22K-Aβ42 was dissolved in 0.1% NH_4OH at 250 μM. After a 10-fold dilution with 50 mM sodium phosphate containing 100 mM NaCl at pH 7.4, the resultant peptide solution (25 μM) was incubated at 37 °C for 48 h. After centrifugation at 21,000*g* at 4 °C,

followed by washing with distilled water, the resultant fibrils were dried in vacuo.

4.5. Transmission electron micrographs of negatively stained preparations of the fibrils formed by E22K-Aβ42 labeled with ^{13}C and ^{15}N

Fibril formation of the E22K-Aβ42 labeled with ^{13}C and ^{15}N was detected by an electron microscope. The incubation conditions were the same as those for preparing the samples for solid-state NMR. Each E22K-Aβ42 peptide was dissolved in 0.1% NH_4OH at 250 μM. After a 10-fold dilution with 50 mM sodium phosphate containing 100 mM NaCl at pH 7.4, the resultant peptide solution (25 μM) was incubated at 37 °C for 48 h. After centrifugation, the supernatant was removed from the pellets. Aggregates were suspended in distilled water by gentle vortex mixing. The suspensions were applied to a 400-mesh collodion-coated copper grid (Nissin EM, Tokyo, Japan) and air-dried before being negatively stained for 2 min with 2% uranyl acetate. The fibrils were examined with the Hitachi H-7500 electron microscope.

4.6. Solid-state NMR experiments

All solid-state NMR experiments were carried out at 9.4 T (100 MHz for ^{13}C) using a Chemagnetics Infinity NMR spectrometer and Chemagnetics 3.2 mm MAS probe at a spinning frequency of 20 kHz and room temperature. The ^{13}C chemical shifts were calibrated in ppm, relative to TMS, by taking the ^{13}C chemical shift for the methine carbon nucleus of solid adamantane (29.5 ppm) as an external reference standard. For the broadband ^{13}C–^{13}C correlation 2D experiment, dipolar-assisted rotational resonance (DARR) was used,[18,19] whose pulse sequence is shown in Figure 4. This pulse sequence began with variable amplitude cross polarization (VACP)[23] using a ramped pulse on the ^{13}C channel. Two pulse phase-modulated (TPPM) decoupling[24] was carried out during the evolution and acquisition periods. After the evolution period, magnetization was placed along the z-axis with a 90° pulse and mixing occurred with a low power ^{1}H recoupling pulse. During mixing time, the ^{1}H radio-frequency field strength was matched to the MAS speed to satisfy the $n = 1$ rotary resonance condition. Pulse sequence parameters of all NMR experiments were; VACP contact time = 0.75 ms, pulse delay = 2 s, TPPM ^{1}H decoupling power = 120 kHz, t_1 increment = 44 μs, and mixing time (τ) = 20 or 500 ms.

Acknowledgments

We thank Dr. Naotaka Izumiyama-Shimomura at Human Tissue Research Group, Tokyo Metropolitan Institute of Gerontology, for the electron microscope. This work was supported in part by Grants-in-Aid for Scientific Research (B) (No. 13460048 and 16380080 to K. I.), for Scientific Research on Priority Areas (No. 17025051 to T. S., T. S., and K. I.), and for the Promotion of Science for Young Scientists (No. 16.1215 to K. M.) from the Ministry of Education, Culture, Sports, Science and Technology of the Japanese Government.

References and notes

1. Selkoe, D. J. *Trends Cell Biol.* **1998**, *8*, 447.
2. Serpell, L. C. *Biochim. Biophys. Acta* **2000**, *1502*, 16.
3. Balbach, J. J.; Petkova, A. T.; Oyler, N. A.; Antzukin, O. N.; Gordon, D. J.; Meredith, S. C.; Tycko, R. *Biophys. J.* **2002**, *83*, 1205.
4. Antzutkin, O. N.; Leapman, R. D.; Balbach, J. J.; Tycko, R. *Biochemistry* **2002**, *41*, 15436.
5. Malinchik, S. B.; Inouye, H.; Szumowski, K. E.; Kirschner, D. A. *Biophys. J.* **1998**, *74*, 537.
6. Tycko, R. *Biochemistry* **2003**, *42*, 3151.
7. Petkova, A. T.; Ishii, Y.; Balbach, J. J.; Antzutkin, O. N.; Leapman, R. D.; Delaglio, F.; Tycko, R. *Proc. Natl. Acad. Sci. U.S.A.* **2002**, *99*, 16742.
8. Wood, S. J.; Wetzel, R.; Martin, J. D.; Hurle, M. R. *Biochemistry* **1995**, *34*, 724.
9. Chou, P. Y.; Fasman, G. D. *J. Mol. Biol.* **1997**, *115*, 135.
10. Morimoto, A.; Irie, K.; Murakami, K.; Ohigashi, H.; Shindo, M.; Nagao, M.; Shimizu, T.; Shirasawa, T. *Biochem. Biophys. Res. Commun.* **2002**, *295*, 306.
11. Morimoto, A.; Irie, K.; Murakami, K.; Masuda, Y.; Ohigashi, H.; Nagao, M.; Fukuda, H.; Shimizu, T.; Shirasawa, T. *J. Biol. Chem.* **2004**, *279*, 52781.
12. Irie, K.; Murakami, K.; Masuda, Y.; Morimoto, A.; Ohigashi, H.; Ohashi, R.; Takegoshi, K.; Nagao, M.; Shimizu, T.; Shirasawa, T. *J. Biosci. Bioeng.* **2005**, *99*, 437.
13. Murakami, K.; Irie, K.; Morimoto, A.; Ohigashi, H.; Shindo, M.; Nagao, M.; Shimizu, T.; Shirasawa, T. *Biochem. Biophys. Res. Commun.* **2002**, *294*, 5.
14. Murakami, K.; Irie, K.; Morimoto, A.; Ohigashi, H.; Shindo, M.; Nagao, M.; Shimizu, T.; Shirasawa, T. *J. Biol. Chem.* **2003**, *278*, 46179.
15. Williams, A. D.; Portelius, E.; Kheterpal, I.; Guo, J.; Cook, K. D.; Xu, Y.; Wetzel, R. *J. Mol. Biol.* **2004**, *335*, 833.
16. Carpino, L. A. *J. Am. Chem. Soc.* **1993**, *115*, 4397.
17. Irie, K.; Oie, K.; Nakahara, A.; Yanai, Y.; Ohigashi, H.; Wender, P. A.; Fukuda, H.; Konishi, H.; Kikkawa, U. *J. Am. Chem. Soc.* **1998**, *120*, 9159.
18. Takegoshi, K.; Nakamura, S.; Terao, T. *Chem. Phys. Lett.* **2001**, *344*, 631.
19. Takegoshi, K.; Nakamura, S.; Terao, T. *J. Chem. Phys.* **2003**, *118*, 2325.
20. Wishart, D. S.; Sykes, B. D. *J. Biomol. NMR* **1994**, *4*, 171.
21. Wiejak, S.; Masiukiewicz, E.; Rzeszotarska, B. *Chem. Pharm. Bull.* **1999**, *47*, 1489.
22. Lajoie, G.; Crivici, A.; Adamon, J. G. *Synthesis* **1990**, 571.
23. Peersen, O. B.; Wu, X.; Smith, S. O. *J. Magn. Reson.* **1994**, *106*, 127.
24. Bennett, A. E.; Rienstra, C. M.; Auger, M.; Lakshmi, K. V.; Griffin, R. G. *J. Chem. Phys.* **1995**, *103*, 6951.
25. Wishart, D. S.; Bigam, C. G.; Holm, A.; Hodges, R. S.; Sykes, B. D. *J. Biomol. NMR* **1995**, *5*, 67.